

The Probabilistic Foundations of Surveillance Failure: From False Alerts to Structural Bias

Marco Pollanen

November 18, 2025

Abstract

For decades, forensic statisticians have debated whether searching large DNA databases undermines the evidential value of a match. Modern surveillance faces an exponentially harder problem: screening populations across thousands of attributes using threshold rules rather than exact matching. Intuition suggests that requiring many coincidental matches should make false alerts astronomically unlikely. This intuition fails.

Consider a system that monitors 1,000 attributes, each with a 0.5 percent innocent match rate. Matching 15 pre-specified attributes has probability 10^{-35} , one in 30 decillion, effectively impossible. But operational systems require no such specificity. They might flag anyone who matches *any* 15 of the 1,000. In a city of one million innocent people, this produces about 226 false alerts. A seemingly impossible event becomes all but guaranteed. This is not an implementation flaw but a mathematical consequence of high-dimensional screening.

We identify fundamental probabilistic limits on screening reliability. Systems undergo sharp transitions from reliable to unreliable with small increases in data scale, a fragility worsened by data growth and correlations. As data accumulate and correlation collapses effective dimensionality, systems enter regimes where alerts lose evidential value even when individual coincidences remain vanishingly rare. This framework reframes the DNA database controversy as a shift between operational regimes. Unequal surveillance exposures magnify failure, making “structural bias” mathematically inevitable. These limits are structural: beyond a critical scale, failure cannot be prevented through threshold adjustment or algorithmic refinement.

Keywords: big data analytics; algorithmic fairness; surveillance systems; DNA databases; false positive rate; Bayesian inference; phase transitions; large deviations theory

1 Introduction

1.1 From Database Search to Threshold Screening

For over two decades, forensic statisticians have debated a fundamental question: does searching a DNA database of a million profiles weaken the evidential value of a match? Stockmarr [1999] argued that database searching increases coincidental match probability, while Balding [2002] maintained that likelihood ratios preserve evidential weight regardless of search method. This controversy (concerning a *single* database with *exact* profile matching) remains unresolved [Storvik, 2006, Kaye, 2013].

Modern surveillance systems face an exponentially harder problem. Rather than searching one database for exact matches, they monitor populations across *thousands* of attributes (locations visited, transactions made, communications sent) and flag individuals whose patterns match *sufficiently many* criteria using a threshold rule rather than exact matching. The intuition that

“requiring many coincidences makes false matches astronomically unlikely” fails catastrophically in this regime.

Consider a concrete example that reveals the nature of this failure. A surveillance system monitors $k = 1000$ binary indicators, each with innocent match probability $p = 0.005$ (half a percent chance), and flags individuals matching at least $m = 15$ attributes. At first glance, this threshold seems extraordinarily conservative. Requiring an exact match across 15 *specific* predetermined attributes would have probability $(0.005)^{15} \approx 3 \times 10^{-35}$, one in 30 decillion). Such exact-match odds suggest false alerts should be astronomically impossible, even across populations of billions.

But operational systems do not require exact matches across 15 predetermined attributes. Instead, they flag individuals matching *at least 15 of any 1000 attributes*. This seemingly subtle distinction changes everything. With $\lambda = kp = 1000 \times 0.005 = 5$ expected chance matches per innocent person and threshold $m = 15$ (three times the expected value), direct calculation gives a per-person false alert probability of

$$q := \Pr(\text{Poisson}(5) \geq 15) \approx 2.26 \times 10^{-4} = 0.0226\%.$$

In a city of $n = 10^6$ innocents, this produces approximately $nq \approx 226$ false alerts, and the probability of at least one false alert is

$$\Pr(\text{at least one false alert}) \approx 1 - e^{-226} \approx 1 - 7 \times 10^{-99}.$$

Thus the probability of *no* false alerts is on the order of 10^{-99} , making the system, for all practical and mathematical purposes, *certain* to flag at least one innocent person.

The “one in 30 decillion” exact-match calculation is mathematically correct but operationally irrelevant. The threshold rule “at least m of k ” transforms the per-person probability from vanishingly small (10^{-35}) to operationally significant (10^{-4}), and population size amplifies this individual-level vulnerability into system-level certainty of failure. This is not a failure of implementation or algorithm design; it is a mathematical inevitability arising from the combinatorics of threshold detection in high-dimensional attribute spaces.

This contrast between the DNA setting and modern multi-attribute surveillance also clarifies why the long-standing DNA database controversy has persisted. Classical DNA searches operate in an extremely sparse false-match regime, where random matches are so rare that enlarging the database does not meaningfully dilute the evidential value of a hit. Multi-attribute threshold screening, however, operates in a dense false-match regime where accumulated coincidences quickly overwhelm the signal. These are mathematically distinct operating regimes; recognizing this distinction resolves the apparent conflict in the DNA literature and motivates the broader probabilistic limits developed in the rest of this paper.

1.2 Main Contributions

This paper develops a rigorous probabilistic framework for analyzing such screening systems. Using classical tools (Poisson approximations, Chernoff bounds, concentration inequalities, and Bayesian inference), we characterize fundamental limits on system reliability. Our analysis reveals that the single-database DNA controversy and multi-attribute surveillance failure are manifestations of the same mathematical phenomenon, differing only in which asymptotic regime they occupy.

Our main contributions include:

1. **Sharp critical population bounds:** We derive two-sided bounds on both per-person and system-level false alert probabilities, showing the critical population grows as $n_{\text{crit}} \asymp \sqrt{\lambda} \exp(\lambda D(c||1))$ with explicit $\sqrt{\lambda}$ corrections (Theorem 2.4). The rate function $D(c||1) = c \log c - c + 1$ governs the exponential scaling.

2. **Finite system lifetimes:** Under exponential data growth $k(t) = k_0\gamma^t$, systems fail at time $T^* \approx \frac{1}{\log \gamma} \log(m/k_0p)$ when $\lambda(t)$ reaches threshold m , with population corrections secondary (Theorem 3.2).
3. **Unified Bayesian-frequentist view:** Both regimes exhibit the same exponential scaling $\exp(\lambda D(c||1))$, but Bayesian actionability requires $n \lesssim \frac{1-\alpha}{\alpha} rs\sqrt{\lambda}e^{\lambda D}$ (for desired PPV $\geq \alpha$) while frequentist reliability allows $n \lesssim \sqrt{\lambda}e^{\lambda D}$ (Section 5). Posterior probabilities collapse when $nq \gg rs$, resolving the Stockmarr-Balding controversy as a regime transition.
4. **Structural bias through group dominance:** Differential surveillance exposure creates exponential outcome disparities that cannot be eliminated through threshold adjustments (Theorems 4.2 through 4.3), formalizing “structural bias” arguments from the algorithmic fairness literature.
5. **Effective dimensionality under correlation:** Spatiotemporal dependencies reduce effective attribute counts to $k_{\text{eff}} \approx A/(2\pi\xi^2)$ (spatial) or $k_{\text{eff}} \approx k/(2\tau)$ (temporal), connecting surveillance analysis to multiple-testing corrections in genomics and neuroimaging (Section 6).

All results use elementary probability theory with proofs provided.

1.3 Motivation and Background

Modern surveillance and screening systems collect vast amounts of data about individuals and attempt to identify rare targets of interest: potential terrorists, criminals, fraudsters, or security threats. These systems operate by comparing observed attributes of individuals (biometric features, transaction patterns, travel histories, communication metadata) against profiles or watchlists, flagging individuals whose patterns match suspiciously well [Lyon, 2003, O’Neil, 2016, Schneier, 2015].

The fundamental challenge is the *curse of dimensionality in coincidence detection*: as monitored attributes grow, innocent individuals increasingly match multiple criteria by chance. When populations are large (millions to billions), even extremely rare coincidences become statistically certain, generating overwhelming false alerts. This parallels challenges in cybersecurity [Axelsson, 2000], where intrusion detection systems with 99.9% accuracy produce unmanageable false alarms when monitoring billions of network flows, and in open-set recognition [Scheirer et al., 2013], where classifiers must distinguish known classes from unknown inputs.

1.4 Related Work and Connections

Our analysis builds on classical probability theory (Poisson approximation, Chernoff bounds, concentration inequalities) applied to modern surveillance contexts. The system-level bound

$$\Pr(\text{false alert}) \approx 1 - (1 - q)^n$$

corresponds to family-wise error rate (FWER) control in multiple testing [Benjamini and Hochberg, 1995, Storey, 2002], though our large-deviation analysis shows when such control becomes infeasible. The base-rate analysis resolves the Stockmarr-Balding debate [Stockmarr, 1999, Balding, 2002] in forensic DNA statistics by identifying distinct asymptotic regimes. Connections to anomaly detection [Axelsson, 2000], open-set recognition [Scheirer et al., 2013], and algorithmic fairness [Hardt et al., 2016, Chouldechova, 2017, Corbett-Davies et al., 2017, Barocas et al., 2019] appear throughout, as false-positive explosion is a fundamental challenge across screening domains.

1.5 The Basic Screening Model

Consider a population of n individuals, each of whom we collect k types of data (e.g., locations visited, financial transactions, etc.). For each type of data, we also have lists of suspicious activity, for example, locations of interest where crimes have occurred. In general, we observe k binary attributes (indicators) for each individual, where each attribute has a small probability $p \ll 1$ of matching some profile of interest purely by chance.

For example, a simple model for the match probability p on the j -th data type might be found by calculating the probability that a person's list (size t) overlaps the suspicious list (size s) on a domain of size V possible distinct items (e.g., V geo-location cells). With uniform sampling without replacement from the domain, the probability of an overlap comes from the zero-intersection hypergeometric probability:

$$p = \Pr(\text{overlap} \geq 1) = 1 - \frac{\binom{V-t}{s}}{\binom{V}{s}} = 1 - \prod_{\ell=0}^{s-1} \left(1 - \frac{t}{V-\ell}\right), \quad \text{for } s \leq V-t,$$

with $p = 1$ when $s > V - t$ (guaranteed overlap).

Now assuming a general model for p , let X_i denote the number of matching attributes for individual i . Under the null hypothesis (individual i is innocent) and the modeling assumptions detailed in Section 1.6, we have:

$$X_i \sim \text{Binomial}(k, p).$$

For large k and small p , we write $\lambda = kp$ for the expected number of chance matches; this parameter will govern all subsequent results.

The screening system flags individual i as suspicious if they match some unsolved crime on m attributes with: $X_i \geq m$ for an integer threshold m (we set $m = \lceil c\lambda \rceil$ later; rounding affects only constant factors). The *per-person false alert probability* is:

$$q = \Pr(X_i \geq m \mid \text{innocent}).$$

Since we screen n individuals, the *system-level false alert probability*, that is, the probability that at least one innocent person is flagged, is:

$$\Pr(\text{at least one false alert}) = 1 - (1 - q)^n.$$

For small q , this is commonly approximated by:

$$\Pr(\text{at least one false alert}) \approx 1 - e^{-nq}.$$

The system becomes *unreliable* when this probability approaches 1 (that is, when $nq \gtrsim 1$), in which case the system is near certain to flag innocent individuals as suspects.

1.6 Modeling Assumptions and Regime of Validity

Throughout this paper, we operate under the following assumptions:

1. **Large- k , small- p regime:** We assume $k \gg 1$ (many attributes), $p \ll 1$ (rare individual matches), with mean $\lambda = kp$ held moderate and fixed as $k \rightarrow \infty$. This is the natural Poisson regime for rare-event detection, where the binomial distribution converges to $\text{Poisson}(\lambda)$ with total-variation error bounded by $2 \sum_{i=1}^k p_i^2$ (see Section 2.1).

2. **Independence across individuals:** The match indicators for different individuals are statistically independent (Remark 2.2). In practice, common-mode events (e.g., mass gatherings, natural disasters) may introduce positive dependence, which would only increase false alert rates beyond our bounds.
3. **Homogeneous match probability (baseline model):** For analytical tractability, we initially assume all attributes have the same match probability p . Section 4 extends to heterogeneous populations with different exposure rates p_g across demographic groups. Remark 2.1 addresses heterogeneity across attributes within individuals.
4. **Binary attributes:** Each attribute either matches ($M = 1$) or doesn't match ($M = 0$) a profile of interest. This models presence/absence at locations, yes/no transaction patterns, or binarized continuous features.
5. **Fixed threshold screening:** The system flags individuals with m or more matches, where m is predetermined. We primarily analyze $m = c\lambda$ for constant $c > 1$, representing thresholds scaled to exceed the expected number of chance matches under the null hypothesis.
6. **Null hypothesis analysis:** We analyze false alerts under the assumption that all n individuals are innocent (the null hypothesis). Detection of actual targets requires separate treatment via signal detection theory and receiver operating characteristic (ROC) analysis [Fawcett, 2006], which is not addressed here. Our results characterize the false positive rate; in practice, system designers must balance this against detection power for true targets.

These assumptions define the scope of our analysis. The core results (Sections 2 through 3) establish fundamental limits under these idealized conditions. Later sections extend the framework: Section 4 analyzes heterogeneous populations with differential exposure, and Section 6 incorporates spatiotemporal correlation structures that reduce the effective dimensionality of attribute spaces.

The large- k , small- p regime is particularly natural for modern surveillance systems, where technological advances enable collection of thousands of binary indicators (GPS pings, transaction flags, communication events), but each individual match remains rare. For instance, with $k = 1000$ location cells and $p = 0.005$ (half-percent chance of presence at any flagged location), we have $\lambda = 5$ expected false matches, a moderate value that falls squarely within our analytical framework.

2 Fundamental Probabilistic Limits

2.1 The Poisson Approximation

When k is large, p is small, and $\lambda = kp$ is *fixed*, the Binomial(k, p) distribution can be approximated by Poisson(λ) [Feller, 1968]. Specifically, if $X \sim \text{Binomial}(k, p)$, then

$$\Pr(X = j) \approx e^{-\lambda} \frac{\lambda^j}{j!}, \quad \lambda = kp.$$

Moreover, by Le Cam's inequality [Barbour et al., 1992],

$$d_{\text{TV}}(\text{Binomial}(k, p), \text{Poisson}(\lambda)) \leq 2 \sum_{i=1}^k p_i^2.$$

For the homogeneous case with $p_i = p$ for all i , this gives $d_{\text{TV}} \leq 2kp^2 = 2\lambda p$. When p is small and $\lambda = kp$ is moderate, this bound is $O(p)$, making the Poisson approximation numerically safe

for practical applications. Throughout, we assume independence across individuals; common-mode shocks would require extensions via positively associated random variables (see Remark 2.2).

Under this approximation, the per-person false alert probability (tail) is

$$q = \Pr(X \geq m) \approx \sum_{j=m}^{\infty} e^{-\lambda} \frac{\lambda^j}{j!} = 1 - \sum_{j=0}^{m-1} e^{-\lambda} \frac{\lambda^j}{j!}.$$

Remark 2.1 (Heterogeneous Attributes). We assume homogeneous match probability p across all attributes for tractability. By Le Cam’s theorem [Barbour et al., 1992], when attributes have varying probabilities p_1, \dots, p_k with $\max_i p_i \rightarrow 0$ and $\lambda = \sum_{i=1}^k p_i$ fixed, the Poisson approximation $d_{\text{TV}}(X, \text{Poisson}(\lambda)) \leq 2 \sum_{i=1}^k p_i^2$ ensures our results depend only on λ , not individual p_i values.

Remark 2.2 (Independence Across Individuals). We use independence across individuals to factor $(1 - q)^n$. In real deployments, common-mode events may introduce positive dependence (positive association means $\Pr(X_i \geq x_i \text{ for all } i) \geq \prod_i \Pr(X_i \geq x_i)$; roughly, variables are more likely to be jointly large than under independence), increasing the system-level false-alert probability. Our bounds hold under independence; extensions to positively associated arrays via Chen-Stein or Stein’s method [Barbour and Chen, 2005] can be derived but are omitted here. Note that positive dependence typically increases tail probabilities (lowers effective rate function), making our independence-based bounds underestimate the true false alert rates when correlation is present.

2.2 Tail Bounds for the Poisson Distribution

To understand how q depends on m and λ , we use Chernoff bounds and related concentration inequalities [Hoeffding, 1963, Mitzenmacher and Upfal, 2005] for Poisson random variables.

Lemma 2.3 (Poisson Upper Tail). *Let $Y \sim \text{Poisson}(\lambda)$ and suppose $m > \lambda$. Then*

$$\Pr(Y \geq m) \leq \left(\frac{e\lambda}{m}\right)^m e^{-\lambda} = \exp\left(-\lambda D\left(\frac{m}{\lambda} \parallel 1\right)\right), \quad (1)$$

where $D(\alpha \parallel 1) = \alpha \log \alpha - \alpha + 1$ is the Poisson rate function (also called the Cramér rate function or Cramér transform of the Poisson distribution with unit mean). This is the Cramér rate function for Poisson random variables, which differs from the binary Kullback-Leibler divergence $D_{\text{KL}}(p \parallel q) = p \log(p/q) + (1 - p) \log((1 - p)/(1 - q))$ used for Bernoulli random variables. The large-deviation rate is asymptotically exact for real $m/\lambda > 1$: the tail probability satisfies $q \asymp \lambda^{-1/2} e^{-\lambda D(m/\lambda \parallel 1)}$ with factorial discreteness contributing only the $\lambda^{-1/2}$ subexponential prefactor. We write $D(c \parallel 1)$ or simply D for brevity when the argument is clear from context.

Proof. For any $t > 0$,

$$\Pr(Y \geq m) = \Pr(e^{tY} \geq e^{tm}) \leq \frac{\mathbb{E}[e^{tY}]}{e^{tm}} = \exp(\lambda(e^t - 1) - tm).$$

Optimizing by setting $\frac{d}{dt}[\lambda(e^t - 1) - tm] = 0$ gives $e^{t^*} = m/\lambda$, which yields the stated bound. \square

2.3 Critical Population Size

We now establish the fundamental scale of population size for reliable screening when the decision threshold scales as $m = c\lambda$ with $c > 1$.

Theorem 2.4 (Critical Population Scale). *Consider a screening system with k binary attributes, per-attribute match probability p , threshold $m = \lceil c\lambda \rceil$ for some $c > 1$, population size n , and $\lambda = kp$. Let $D(c\|1) = c \log c - c + 1$ (the Poisson rate function from Lemma 2.3). Then the per-person false alert probability q satisfies the following asymptotic bounds:*

$$\frac{1}{\sqrt{2\pi c\lambda}} \exp\left(-\lambda D(c\|1) - \frac{1}{12c\lambda}\right) \leq q \leq \exp(-\lambda D(c\|1)), \quad (2)$$

which hold for $\lambda \geq 1$ and $c > 1$ with the stated constants; for smaller λ the same exponential form holds with different absolute constants. The system-level false alert probability obeys

$$1 - \exp\left(-\frac{n}{\sqrt{2\pi c\lambda}} e^{-\lambda D(c\|1) - \frac{1}{12c\lambda}}\right) \leq \Pr(\text{false alert}) \leq 1 - \exp\left(-\frac{n e^{-\lambda D(c\|1)}}{1 - e^{-\lambda D(c\|1)}}\right). \quad (3)$$

(For $e^{-\lambda D} \leq 1/2$, the upper bound denominator is within a factor of 2 in the exponent, providing tight control.) In particular, the system becomes unreliable once

$$n \gtrsim \sqrt{\lambda} \exp(\lambda D(c\|1)) \quad (\text{up to constant factors}),$$

and the critical population scale is

$$n_{\text{crit}} \asymp \exp(\lambda D(c\|1)) = \exp(kp D(c\|1)), \quad (4)$$

ignoring subexponential $\sqrt{\lambda}$ corrections. Here we use the notation $f \asymp g$ to denote equality up to multiplicative constants independent of the main asymptotic parameters (λ, k, n) .

Proof. Take $m = \lceil c\lambda \rceil$ with $c > 1$; replacing m by $c\lambda$ (ignoring rounding) affects only constants in the bounds. The upper bound in (2) is Lemma 2.3 with $m = c\lambda$: $q \leq \exp(-\lambda D(c\|1))$.

The lower bound follows from Robbins' refinement of Stirling's formula $m! < \sqrt{2\pi m} \left(\frac{m}{e}\right)^m e^{\frac{1}{12m}}$ [Robbins, 1955].

$$\Pr(Y = m) = e^{-\lambda} \frac{\lambda^m}{m!} \geq \frac{1}{\sqrt{2\pi m}} \exp\left(-\lambda + m \log \lambda - m \log m + m - \frac{1}{12m}\right).$$

Setting $m = c\lambda$ gives

$$\Pr(Y = m) \geq \frac{1}{\sqrt{2\pi c\lambda}} \exp\left(-\lambda D(c\|1) - \frac{1}{12c\lambda}\right),$$

since

$$-\lambda + m \log(\lambda/m) + m = -\lambda [c \log c - c + 1] = -\lambda D(c\|1).$$

Since $q = \Pr(Y \geq m) \geq \Pr(Y = m)$, the same lower bound applies to q .

For the system-level probability, independence across n individuals gives $\Pr(\text{no false alert}) = (1 - q)^n$ and thus $\Pr(\text{false alert}) = 1 - (1 - q)^n$.

Since $e^t \geq 1 + t$ for all $t \in \mathbb{R}$, substituting $t = \frac{x}{1-x}$ (valid for $x \in [0, 1)$) gives

$$1 - x = \frac{1}{1+t} \geq e^{-t} = e^{-x/(1-x)},$$

and thus (by $\ln(1-x) \leq -x$ and $\ln(1-x) \geq -x/(1-x)$ for $x \in (0, 1)$),

$$e^{-q/(1-q)} \leq 1 - q \leq e^{-q},$$

so on the system level:

$$1 - e^{-nq} \leq 1 - (1 - q)^n \leq 1 - e^{-nq/(1-q)}.$$

Together with the bounds on q above yields the bounds in (3). The factor $1/(1 - q)$ in the upper bound arises from the inequality $(1 - q)^n \geq e^{-nq/(1-q)}$; since $q \leq e^{-\lambda D}$, we have $q/(1 - q) \leq e^{-\lambda D}/(1 - e^{-\lambda D})$, which gives the stated upper bound. When $q \leq e^{-\lambda D}$ is small, $1 - q \geq 1 - e^{-\lambda D}$ provides a uniform lower bound independent of n .

The system is *unreliable* when the exponent in the lower bound becomes $O(1)$ (that is, when the expected number of false alerts per batch is on the order of one):

$$\frac{n}{\sqrt{2\pi c\lambda}} e^{-\lambda D(c\|1) - \frac{1}{12c\lambda}} \approx 1.$$

Solving for n gives

$$n_{\text{crit}} \approx \sqrt{2\pi c\lambda} e^{\lambda D(c\|1) + \frac{1}{12c\lambda}}.$$

The $\frac{1}{12c\lambda}$ term is tiny for large λ , so asymptotically we write

$$n_{\text{crit}} \asymp \sqrt{\lambda} e^{\lambda D(c\|1)},$$

or for rough scaling (ignoring the $\sqrt{\lambda}$ factor):

$$n_{\text{crit}} \asymp e^{\lambda D(c\|1)} = e^{kpD(c\|1)}.$$

That is, the *critical population size* beyond which false alerts almost surely occur. \square

Remark 2.5 (Numerical Validation). Monte Carlo simulations (5000 runs per data point) validate the Poisson approximation and system-level probability model: simulated false-alert rates match theoretical predictions with mean absolute error of 0.0015 across the critical transition region (Figure 1(a)). The sharp threshold behavior predicted by Proposition 2.6 is clearly evident in the simulation data.

2.4 Sharp Threshold Behavior

The relationship between population size and system reliability exhibits an increasingly sharp threshold as the number of attributes grows.

Proposition 2.6 (Threshold Sharpness). *Consider a screening system with $\lambda = kp$, threshold $m = c\lambda$ for fixed $c > 1$, and population scaled as $n = \sqrt{\lambda} \cdot e^{\alpha\lambda D(c\|1)}$ for $\alpha > 0$. Then the system-level false alert probability satisfies:*

$$\lim_{\lambda \rightarrow \infty} \Pr(\text{false alert}) = \begin{cases} 0 & \text{if } \alpha < 1, \\ 1 & \text{if } \alpha > 1. \end{cases} \quad (5)$$

The transition occurs in a window $\Delta\alpha \sim 1/(\lambda D(c\|1)) \rightarrow 0$, becoming arbitrarily sharp as λ increases. This follows from standard large-deviation theory for sums of i.i.d. rare events [Dembo and Zeitouni, 2010].

Proof. From Theorem 2.4, we have the two-sided bounds

$$\frac{1}{\sqrt{2\pi c\lambda}} e^{-\lambda D(c\|1) - O(1/\lambda)} \leq q \leq e^{-\lambda D(c\|1)},$$

which together imply $\log q = -\lambda D(c\|1) + O(\log \lambda)$ as $\lambda \rightarrow \infty$ (since $q \geq C\lambda^{-1/2}e^{-\lambda D}$ and $q \leq e^{-\lambda D}$, taking logarithms gives the stated error term). With $n = \sqrt{\lambda}e^{\alpha\lambda D(c\|1)}$, we have

$$\log(nq) = \log n + \log q = \frac{1}{2} \log \lambda + \alpha\lambda D(c\|1) - \lambda D(c\|1) + O(\log \lambda),$$

which simplifies to

$$\log(nq) = (\alpha - 1)\lambda D(c\|1) + O(\log \lambda).$$

Hence for $\alpha < 1$, $nq \rightarrow 0$ exponentially; for $\alpha > 1$, $nq \rightarrow \infty$ exponentially. The transition width $\Delta\alpha$ satisfying $|(\alpha - 1)\lambda D| = O(1)$ gives $\Delta\alpha = O(1/(\lambda D))$, which vanishes as $\lambda \rightarrow \infty$. Equivalently, the absolute window in $\log n$ is $O(1)$, making the transition arbitrarily sharp in the exponential scale. The limiting behavior (5) follows from $\Pr(\text{false alert}) \approx 1 - e^{-nq}$, which approaches 0 when $nq \rightarrow 0$ and approaches 1 when $nq \rightarrow \infty$. \square

Remark 2.7. This sharp threshold implies no gradual degradation: systems operating near the critical line $\log n = \lambda D(c\|1)$ transition from reliable to unreliable essentially instantaneously as λ increases (Figure 1). Combined with exponential data growth $\lambda(t) = \lambda_0\gamma^t$, every system inevitably crosses this threshold at finite time $T^* \sim \log(m/\lambda_0)/\log \gamma$ (Theorem 3.2), making failure predictable rather than merely possible.

3 Temporal Dynamics: Finite System Lifetimes

Real surveillance systems accumulate data over time. As more attributes are collected, the false alert problem intensifies until the system becomes unreliable. We now quantify how long a screening system can operate before this inevitable failure occurs. As Figure 1(c) demonstrates, systems with exponential data growth exhibit sharp temporal transitions from reliable to unreliable operation at predictable times.

Remark 3.1 (Change of Threshold Regime). In the preceding analysis (Section 2), we studied thresholds of the form $m = c\lambda$ with $c > 1$ constant, where both m and λ scale together. In this section, we adopt a different perspective: we fix the threshold m at deployment time while allowing $\lambda(t) = k(t) \cdot p$ to grow over time as data accumulates. This models realistic system operation, where detection thresholds are predetermined policy parameters that remain constant even as surveillance capabilities expand. The critical behavior occurs when the growing $\lambda(t)$ crosses the fixed threshold m , at which point false alerts become inevitable.

3.1 Exponential Data Growth

Modern data collection exhibits exponential growth [Hilbert and López, 2011]. We model this as:

$$k(t) = k_0\gamma^t, \tag{6}$$

where k_0 is the initial number of monitored attributes at time $t = 0$, and $\gamma > 1$ is the growth factor per time unit (e.g., annual growth rate).

Since each attribute has probability p of matching by chance for an innocent individual, the expected number of false matches grows exponentially:

$$\lambda(t) = k(t) \cdot p = k_0p \cdot \gamma^t. \tag{7}$$

3.2 Critical Time Derivation

The system flags an individual when they have m or more matching attributes. At time t , the per-person false alert probability is:

$$q(t) = \Pr(\text{Poisson}(\lambda(t)) \geq m).$$

With population size n , the probability of at least one false alert is approximately:

$$\Pr(\text{system false alert at time } t) \approx 1 - e^{-n \cdot q(t)}.$$

The system becomes unreliable when $n \cdot q(t) \gtrsim 1$.

Theorem 3.2 (System Lifetime Under Exponential Growth). *Consider a screening system with exponential data growth $k(t) = k_0 \gamma^t$ (where $\gamma > 1$), per-attribute match probability p , fixed threshold m , and population size n .*

For populations large enough that system failure occurs near $\lambda(T^) \approx m$ (rather than deep in the Poisson tail), the system becomes unreliable at time*

$$T^* \approx \frac{1}{\log \gamma} \log \left(\frac{m}{k_0 p} \right), \quad (8)$$

where the critical time is characterized by $\lambda(T^*) \approx m$.

The population size n introduces a correction of order $\frac{1}{\log \gamma} \sqrt{\frac{\log n}{m}}$ to the time to failure (equivalently, a shift of order $\sqrt{2m \log n}$ in λ), up to logarithmic factors in m and n . This is typically weak relative to the effects of γ and m .

Proof sketch. The system fails when the expected number of false alerts reaches order one: $n \cdot q(T^*) \sim 1$. For $\lambda < m$, the Poisson tail probability $q(\lambda) = \Pr(\text{Poisson}(\lambda) \geq m)$ is exponentially suppressed by the factor $\exp(-\lambda D(m/\lambda|1))$. As λ increases from well below m toward m , the rate function $D(m/\lambda|1)$ decreases to zero, causing $q(\lambda)$ to increase sharply from nearly zero to order one. When $\lambda > m$, the tail probability increases rapidly toward 1. The transition occurs sharply near $\lambda = m$ due to concentration of the Poisson distribution.

For λ near m , we use the normal approximation $\text{Poisson}(\lambda) \approx N(\lambda, \lambda)$, which yields $q(\lambda) = \Pr(X \geq m) \approx 1 - \Phi((m - \lambda)/\sqrt{\lambda})$. For $\lambda \lesssim m$, the Gaussian tail asymptotics (Mills' ratio: $1 - \Phi(x) \sim \phi(x)/x$ as $x \rightarrow \infty$) give the more precise form:

$$q(\lambda) \sim \frac{\sqrt{\lambda}}{(m - \lambda)\sqrt{2\pi}} e^{-(m-\lambda)^2/(2\lambda)} \quad (\lambda < m).$$

Setting $nq(T^*) \sim 1$ gives $\lambda(T^*) \approx m - \sqrt{2m \log n}$, which is a small correction to $\lambda(T^*) = m$ for typical parameters. Translating through $\lambda(t) = k_0 p \gamma^t$ yields a time shift of order $\frac{1}{\log \gamma} \sqrt{\frac{\log n}{m}}$. Substituting into $\lambda(t) = k_0 p \gamma^t$ yields (8) as the leading-order term. \square

3.3 Key Insights

Equation (8) reveals several fundamental properties:

1. **Finite lifetime is inevitable:** For any fixed threshold m and exponential growth $\gamma > 1$, we have $T^* < \infty$. Even if one attempted to maintain reliability by scaling the threshold with data ($m \propto \lambda(t)$), this would require the monitored population to grow as $n_{\text{crit}}(t) \sim \exp(c\gamma^t)$, doubly-exponential growth that far exceeds realistic population dynamics. Real surveillance systems use fixed thresholds and monitor approximately fixed populations, making temporal failure inevitable. [This mathematical structure parallels the “double birthday paradox” analysis of Pollanen [2024], though arising here in a distinct screening context.]
2. **Logarithmic dependence on threshold:** Doubling the threshold m adds only $(\log 2)/\log \gamma$ time units. For annual doubling ($\gamma = 2$), this is exactly 1 year. Even increasing m tenfold extends lifetime by only $\log_2(10) \approx 3.3$ years.
3. **Inverse dependence on growth rate:** The factor $1/\log \gamma$ means faster data growth dramatically reduces system lifetime. Increasing γ from 1.5 to 2 (from 50% to 100% annual growth) roughly halves the operational lifetime.
4. **Weak population dependence:** While larger populations cause slightly earlier failure, this effect is logarithmic in n and secondary to the exponential effects of γ and m . The system lifetime is primarily determined by data growth dynamics, not population size.

The temporal phase transition in Figure 1(c) illustrates these dynamics: a system with 50% annual growth ($\gamma = 1.5$) operates reliably for approximately 4 years before crossing the critical threshold, after which false alerts become statistically inevitable.

3.4 Quantitative Examples

Example 3.3 (Border Security System). Consider a border security system with initial attributes $k_0 = 100$, annual growth rate $\gamma = 1.5$ (50%), match probability $p = 0.01$, and threshold $m = 5$. The critical time is:

$$T^* = \frac{\log(5/(100 \times 0.01))}{\log 1.5} = \frac{\log 5}{\log 1.5} \approx 4.0 \text{ years.}$$

The lifetime sensitivity reveals fundamental constraints. Increasing m from 3 to 10:

$$T^*(m = 3) = \frac{\log(3/(100 \times 0.01))}{\log 1.5} = \frac{\log 3}{\log 1.5} \approx 2.7 \text{ years,}$$

$$T^*(m = 10) = \frac{\log(10/(100 \times 0.01))}{\log 1.5} = \frac{\log 10}{\log 1.5} \approx 5.7 \text{ years.}$$

Increasing the threshold from 3 to 10 extends lifetime from 2.7 to only 5.7 years (logarithmic benefit). In contrast, doubling γ from 1.5 to 2.0:

$$T^*(m = 5, \gamma = 2.0) = \frac{\log 5}{\log 2} \approx 2.3 \text{ years,}$$

cuts lifetime nearly in half (from 4.0 to 2.3 years). Growth rate dominates system longevity; threshold adjustments provide minimal protection.

3.5 Practical Implications

1. **Predictable obsolescence:** Every system has a calculable expiration date $T^* \sim \frac{1}{\log \gamma} \log(m/k_0 p)$. Monitoring $\lambda(t)/m$ provides early warning.

2. **Growth rate dominates:** Lifetime scales as $1/\log \gamma$; doubling γ halves operational lifetime. Threshold adjustments provide only logarithmic benefit.

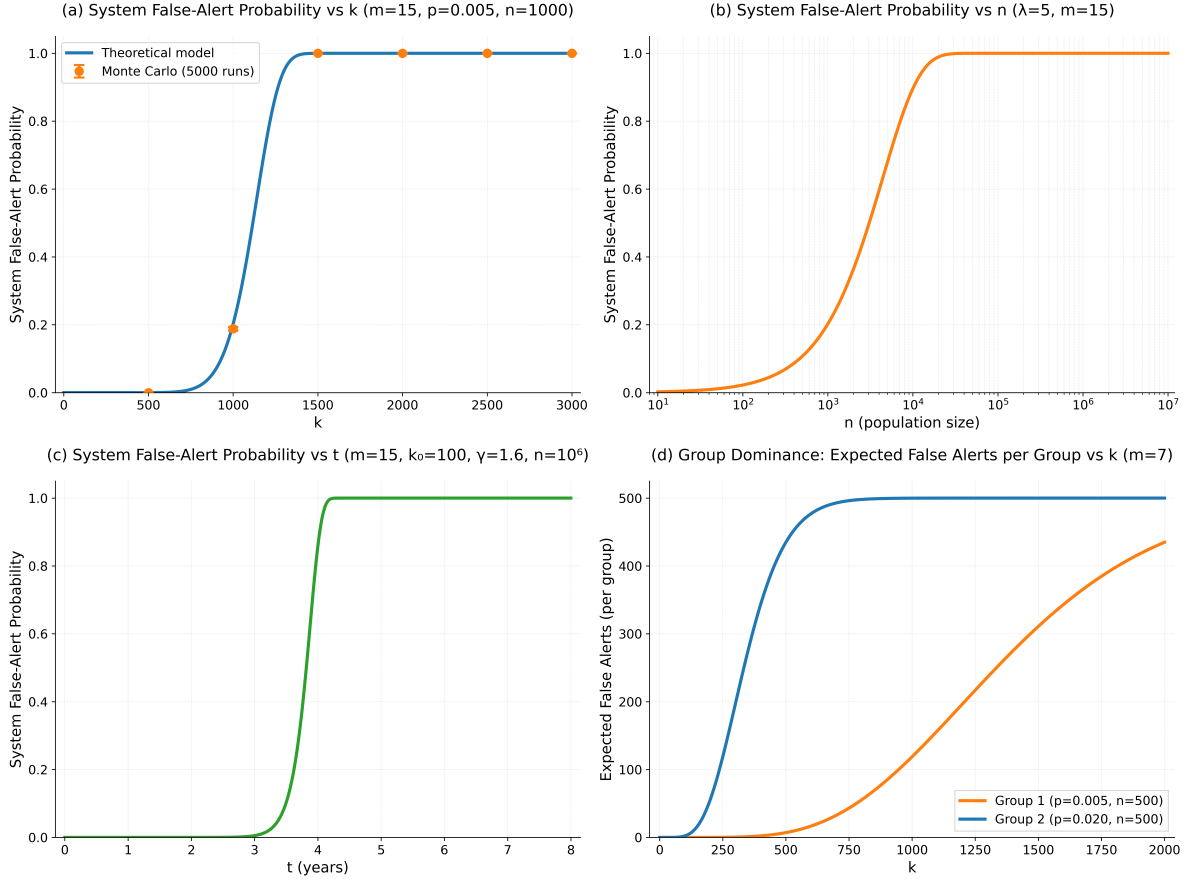


Figure 1: **Phase transitions in surveillance system reliability.** Systems exhibit sharp transitions from reliable to unreliable operation across four dimensions: (a) attribute growth with Monte Carlo validation (orange points, 5000 runs) confirming theoretical predictions (mean error < 0.002), (b) population scaling ($\log n$ vs. false-alert probability), (c) temporal dynamics (t vs. false-alert probability under exponential data growth), and (d) group dominance showing differential exposure creates exponential false-alert disparities. All transitions sharpen as system parameters increase, consistent with large-deviation theory.

4 Heterogeneous Population Structure

Not all individuals have equal representation in surveillance databases. Socioeconomic, geographic, and demographic factors lead to differential exposure rates [Lyon, 2003, Eubanks, 2018].

4.1 Multi-Group Model

Partition the population into G groups, such that group g has n_g individuals, with $\sum_{g=1}^G n_g = n$, and each individual in group g has per-attribute match probability p_g . Let $\lambda_g = kp_g$ and define

the per-group false alert probability:

$$q_g = \Pr(\text{Poisson}(\lambda_g) \geq m).$$

Proposition 4.1 (Heterogeneous System Risk). *The system-level false alert probability is:*

$$\Pr(\text{false alert}) = 1 - \prod_{g=1}^G (1 - q_g)^{n_g} \approx 1 - \exp\left(-\sum_{g=1}^G n_g q_g\right). \quad (9)$$

Proof. The events “individual i in group g generates a false alert” are independent across individuals. The probability that no one in group g alerts is $(1 - q_g)^{n_g}$. Since groups are disjoint, the probability that no one alerts is the product over groups. The approximation follows from $(1 - x)^n \approx e^{-nx}$ for small x . \square

4.2 Dominance and Disparity

Theorem 4.2 (Group Dominance Effect: Algebraic Decomposition). *Let $g^* = \arg \max_g \{n_g q_g\}$ be the group contributing the most to system risk. Then:*

$$\Pr(\text{false alert}) \approx 1 - e^{-n_{g^*} q_{g^*}} + O\left(\left(\sum_{g \neq g^*} n_g q_g\right) e^{-n_{g^*} q_{g^*}}\right). \quad (10)$$

If $n_{g^} q_{g^*} \gg \sum_{g \neq g^*} n_g q_g$, then group g^* dominates system behavior. This is an algebraic decomposition showing how system-level risk concentrates in the highest-exposure group.*

Proof. From Proposition 4.1:

$$1 - \exp\left(-\sum_{g=1}^G n_g q_g\right) = 1 - \exp(-n_{g^*} q_{g^*}) \cdot \exp\left(-\sum_{g \neq g^*} n_g q_g\right).$$

Using $e^{-x} \approx 1 - x$ for small x :

$$\begin{aligned} &\approx 1 - e^{-n_{g^*} q_{g^*}} \left(1 - \sum_{g \neq g^*} n_g q_g\right) \\ &= 1 - e^{-n_{g^*} q_{g^*}} + e^{-n_{g^*} q_{g^*}} \sum_{g \neq g^*} n_g q_g. \end{aligned}$$

The main term is $1 - e^{-n_{g^*} q_{g^*}}$, representing the contribution from group g^* . The correction term is of order $(\sum_{g \neq g^*} n_g q_g) e^{-n_{g^*} q_{g^*}}$ and becomes negligible whenever $n_{g^*} q_{g^*} \gg \sum_{g \neq g^*} n_g q_g$. \square

4.3 Fairness Implications

The Group Dominance Effect (Theorem 4.2) has important implications for fairness in surveillance systems. When different population groups experience differential surveillance exposure, small differences in exposure rates create exponential disparities in outcomes. Proposition 4.3 shows that exposure ratios of 2–4 times generate false alert disparities exceeding 20 times near critical thresholds, due to Poisson tail behavior. This exponential amplification means that even modest differences in surveillance intensity produce severe outcome inequalities.

Crucially, these disparities cannot be eliminated through threshold adjustment. Group-specific thresholds merely encode the underlying exposure inequality in a different form. Equalizing outcomes requires equalizing data collection intensity at the source, not algorithmic tuning. Moreover, since the high-exposure group drives system-level false alerts, aggregate reliability metrics obscure concentrated burdens on specific subpopulations, making demographic disaggregation essential for understanding actual system performance.

Proposition 4.3 (Exposure Amplification Through Poisson Tails). *Consider two groups with equal population size ($n_1 = n_2 = n/2$) but different per-attribute match probabilities $p_1 < p_2$. Let $\lambda_i = kp_i$ and suppose both groups are screened with common threshold m . Then:*

1. *If $\lambda_1 < m \leq \lambda_2$, the disparity in expected false alerts is exponential:*

$$\frac{n_2 q_2}{n_1 q_1} = \frac{q_2}{q_1} \geq \exp(c \cdot m) \quad (11)$$

for some constant $c > 0$ (depending on λ_1), for all sufficiently large m . (Since $q_1 \lesssim (\lambda_1/m)^m$ for $m > \lambda_1$, while $q_2 \geq 1/2 - O(m^{-1/2})$ by the central limit theorem, the ratio q_2/q_1 grows super-exponentially in m . In particular, for any fixed constant $c > 0$ there exists $M(c)$ such that for all $m \geq M(c)$,

$$\frac{q_2}{q_1} \geq \exp(cm).$$

Thus the disparity eventually dominates $\exp(cm)$ for arbitrary but fixed $c > 0$.) Indeed, $q_2 \geq \Pr(\text{Poisson}(m) \geq m)$ by monotonicity, and for large m , $\Pr(\text{Poisson}(m) \geq m) \geq 1/2 - O(m^{-1/2})$, while $q_1 \leq \exp(-\lambda_1 D(m/\lambda_1 \| 1))$ by the Chernoff bound in Lemma 2.3, which is exponentially small for $m > \lambda_1$.

2. *The fraction of false alerts attributable to Group 2 approaches 1 as the exposure gap grows:*

$$\frac{n_2 q_2}{n_1 q_1 + n_2 q_2} \rightarrow 1 \quad \text{as } \lambda_2 - m \text{ increases.}$$

3. *For fixed threshold m and exposure ratio $\alpha = p_2/p_1 > 1$, as k increases, Group 2 enters the critical regime ($\lambda_2 \approx m$) before Group 1, creating a temporal window of maximum disparity.*

Proof. (1) When $\lambda_2 \geq m$, by monotonicity of the Poisson tail probability in the parameter λ , we have

$$q_2 = \Pr(\text{Poisson}(\lambda_2) \geq m) \geq \Pr(\text{Poisson}(m) \geq m).$$

For large m , by symmetry of the limiting normal approximation, $\Pr(\text{Poisson}(m) \geq m)$ approaches $1/2$ from below. The median of the $\text{Poisson}(m)$ distribution satisfies $m - \log 2 \leq \text{median} \leq m + 1/3$, so the tail probability at m is bounded below by $1/2 - O(m^{-1/2})$. Meanwhile, $q_1 \leq \exp(-\lambda_1 D(m/\lambda_1 \| 1))$ by Lemma 2.3, which is exponentially small when $m > \lambda_1$. The ratio q_2/q_1 therefore grows at least exponentially in m : for some constant $c > 0$ (depending on λ_1), we have $q_2/q_1 \geq \exp(c \cdot m)$ for sufficiently large m .

(2) Follows from (1) by noting $q_2/(q_1 + q_2) \rightarrow 1$ when $q_2/q_1 \rightarrow \infty$.

(3) Group 2 reaches $\lambda_2 = m$ when $k = m/p_2$, while Group 1 reaches $\lambda_1 = m$ when $k = m/p_1 > m/p_2$. The disparity is maximal in the interval $m/p_2 < k < m/p_1$. \square

Remark 4.4 (Structural vs. Algorithmic Bias). Proposition 4.3 demonstrates that disparate outcomes arise from the *probabilistic structure* of screening systems, independent of algorithmic design choices. When different groups experience differential surveillance exposure rates ($p_1 \neq p_2$), this

mathematically guarantees unequal false positive rates ($q_1 \neq q_2$) under any common threshold m , creating disproportionate false alert burdens through Poisson tail behavior.

The exponential amplification in part (1) is particularly striking: when both groups are screened using the same attribute set and threshold, small differences in exposure translate to exponential differences in false alert rates (Figure 1(d)). The effect manifests temporally as different groups reach critical false-alert rates at different times: Group 2 with exposure rate $p_2 = 0.020$ fails at $k_2^* = 350$ attributes, while Group 1 with $p_1 = 0.005$ remains reliable until $k_1^* = 1400$. This fourfold difference in system lifetime arises from the fourfold difference in exposure rates, but the amplification becomes exponential when comparing simultaneous false alert rates: at intermediate $k \in (350, 1400)$, Group 2 experiences exponentially more false alerts than Group 1.

Our exponential disparity result formalizes concerns from the algorithmic fairness literature about the inadequacy of threshold-based fairness metrics [Hardt et al., 2016, Barocas et al., 2019]. Even attempting to equalize false positive rates through group-specific threshold adjustments cannot eliminate outcome disparities, as the required thresholds themselves encode the underlying exposure inequalities. This suggests fairness cannot be achieved through algorithmic tuning alone [Dwork et al., 2012], but requires equalizing data collection intensity at the source. This conclusion extends recent work on “fairness through awareness” and formalizes “structural bias” arguments [Eubanks, 2018, Benjamin, 2019] showing that disparities are intrinsic to systems built on heterogeneous data collection, not merely implementation artifacts.

4.4 Numerical Example: Geographic Disparities

Consider a city with two neighborhoods:

- Neighborhood A (low surveillance): $n_A = 100,000$, $p_A = 0.005$
- Neighborhood B (high surveillance): $n_B = 100,000$, $p_B = 0.02$

With $k = 100$ attributes and threshold $m = 3$:

$$\lambda_A = 100 \cdot 0.005 = 0.5, \quad q_A = \sum_{j=3}^{\infty} e^{-0.5} \frac{0.5^j}{j!} \approx 0.014,$$

$$\lambda_B = 100 \cdot 0.02 = 2, \quad q_B = \sum_{j=3}^{\infty} e^{-2} \frac{2^j}{j!} \approx 0.323.$$

Expected number of false alerts:

$$n_A q_A \approx 100,000 \cdot 0.014 = 1,400,$$

$$n_B q_B \approx 100,000 \cdot 0.323 = 32,300.$$

Despite equal population sizes, Neighborhood B experiences approximately 23 times more false alerts. This exponential disparity, visualized in Figure 1(d), demonstrates how differential exposure rates create fundamentally unequal outcomes that cannot be remedied through threshold adjustments alone. Moreover, by Theorem 4.2, since $n_B q_B \gg n_A q_A$, the system-level false alert probability is dominated by Neighborhood B:

$$\Pr(\text{system false alert}) \approx 1 - e^{-32,300} \approx 1.$$

The system is essentially guaranteed to produce false alerts, driven almost entirely by the heavily surveilled neighborhood. This illustrates how heterogeneous exposure not only creates disparate individual-level burdens but also determines aggregate system reliability.

Remark 4.5 (Policy Implications). These results suggest that surveillance system audits should:

1. Measure exposure rates (p_g) across demographic and geographic groups, not just aggregate false alert rates.
2. Recognize that *system reliability is bounded by the worst-performing group* (Theorem 4.2), making demographic disaggregation essential.
3. Account for temporal dynamics: groups with higher exposure fail first as data accumulates, creating windows of maximum disparity.
4. Acknowledge that threshold adjustments cannot eliminate disparities arising from differential exposure; only equalizing p_g across groups can achieve fairness.

5 Bayesian Posterior Reliability and the Base-Rate Trap

The preceding analysis focused on frequentist system reliability: the probability that at least one innocent individual is flagged. However, practitioners ultimately need the *posterior probability* that a flagged person is truly a target. This Bayesian perspective reveals an even more stringent constraint: in the sparse-target regime (where the expected number of true targets r is small relative to population size), posterior reliability degrades once nq becomes comparable to rs , and collapses when $nq \gg rs$. In this regime, flags become epistemically meaningless well before the frequentist transition at $nq \sim 1$.

5.1 The Bayesian Framework and Positive Predictive Value

We introduce standard notation from diagnostic testing and forensic statistics [Balding, 2002]:

$$\begin{aligned} \pi &\equiv \Pr(\text{target}) \quad (\text{base rate}), \\ s &\equiv \Pr(\text{flag} \mid \text{target}) \quad (\text{sensitivity}), \\ q &\equiv \Pr(\text{flag} \mid \text{innocent}) \quad (\text{false positive rate}). \end{aligned}$$

By Bayes' rule, the *positive predictive value (PPV)* is

$$\Pr(\text{target} \mid \text{flag}) = \frac{s \pi}{s \pi + q (1 - \pi)}. \tag{12}$$

In a screened population of size n with r true targets ($\pi = r/n$), the expected number of flagged individuals is:

$$\mathbb{E}[\# \text{ flags}] \approx r s + n q.$$

Thus, the expected false discovery rate (FDR) is

$$\text{FDR} \approx \frac{n q}{r s + n q}, \quad \text{PPV} = 1 - \text{FDR} \approx \frac{r s}{r s + n q}, \tag{13}$$

matching (12) exactly.

5.2 Posterior Reliability and Bayesian Critical Scales

In the large-deviation setting of Theorem 2.4, with threshold $m = c\lambda$ and $c > 1$, the false positive rate satisfies

$$q \asymp \kappa(\lambda) e^{-\lambda D(c\|1)}, \quad \kappa(\lambda) = O(\lambda^{-1/2}),$$

up to subexponential prefactors. Combining this with (13) yields an explicit condition for maintaining actionable posterior probabilities.

Proposition 5.1 (Bayesian Critical Population for Actionable PPV). *Fix a desired posterior level $\alpha \in (0, 1)$ (e.g., $\alpha = 0.9$) and sensitivity $s \in (0, 1]$. Let r denote the expected number of true targets in the population (so the base rate is $\pi = r/n$). In the sparse-target regime where r is fixed or grows sublinearly with n , the condition*

$$\Pr(\text{target} \mid \text{flag}) \geq \alpha$$

is satisfied whenever

$$n \leq \frac{(1 - \alpha) r s}{\alpha q}. \quad (14)$$

Under the large-deviation scaling $q \asymp \kappa(\lambda) e^{-\lambda D(c\|1)}$, the Bayesian critical population size satisfies

$$n_{\text{crit}}^{\text{Bayes}}(\alpha, s) \asymp \frac{(1 - \alpha) r s}{\alpha} \sqrt{\lambda} \exp(\lambda D(c\|1)), \quad (15)$$

where \asymp hides subexponential factors absorbed into $\kappa(\lambda)$.

Remark 5.2 (Regime of Validity). Proposition 5.1 applies to the “needle in a haystack” setting where r is fixed or grows slowly while n increases. If instead $r \propto n$ (constant prevalence), then the ratio r/n is fixed, and the condition for actionable PPV reduces to a bound on q/s relative to $\alpha/(1 - \alpha)$, independent of n . The sparse-target regime is the most challenging case for screening systems and is therefore the primary focus of this analysis.

Proof. From (13), $\text{PPV} \geq \alpha$ iff $r s \geq \alpha(r s + n q)$. Rearranging gives $r s(1 - \alpha) \geq \alpha n q$, which yields (14). Substituting the large-deviation scaling for q proves (15). \square

Remark 5.3 (The Bayesian Trap). Frequentist reliability deteriorates once $nq \sim 1$, when the system is likely to produce at least one false alert. Bayesian actionability demands the stronger condition $nq \ll rs$. When $rs > 1$, there is an intermediate regime where false alerts occur frequently but individual flags retain some evidential value. When $rs < 1$ (extremely sparse targets), posterior reliability collapses before the system becomes statistically unreliable. In all cases, if $nq \gg rs$, posterior probabilities decay toward zero even when individual false positives remain rare.

5.3 Likelihood Ratios and Classical Fallacies

Analysts often cite tiny false positive rates q or large likelihood ratios

$$L = \frac{s}{q},$$

and mistakenly infer that $\Pr(\text{target} \mid \text{flag})$ is therefore large. This is the classical *prosecutor’s fallacy* [Balding, 2002]. Bayes’ rule shows:

$$\frac{\Pr(\text{target} \mid \text{flag})}{\Pr(\text{innocent} \mid \text{flag})} = \frac{s}{q} \cdot \frac{\pi}{1 - \pi} = L \times \text{prior odds}. \quad (16)$$

When the base rate $\pi = r/n$ is small, the prior odds can overwhelm any fixed likelihood ratio. Even extremely rare false positives ($q \ll 1$) do not guarantee high PPV. When $\pi \ll q$, most flagged individuals remain innocent despite individually low false positive rates.

5.4 Resolving the DNA Database Controversy

Forensic statisticians have long debated the evidential value of DNA “cold hits.” Stockmarr [1999] argued that searching databases weakens evidence by inflating coincidental match probabilities; Balding and Donnelly [1995], Balding [2002] countered that likelihood ratios preserve evidential weight. Our framework resolves the debate.

Using (16),

$$\frac{\Pr(\text{guilty} \mid \text{match})}{\Pr(\text{innocent} \mid \text{match})} = \frac{s}{q} \cdot \frac{r/n}{1 - r/n}.$$

Standard STR genotype profiling yields match probabilities on the order of $q \sim 10^{-12}$ or smaller. Even with databases of size $n \sim 10^6$, the product $nq \sim 10^{-6} \ll 1$ remains far below the critical scale where coincidental matches become probable. In this extreme regime, likelihood ratios dominate the posterior odds, validating Balding’s argument that database size does not meaningfully dilute evidential weight.

By contrast, multi-attribute surveillance systems often operate far above the critical threshold, where prior odds collapse faster than likelihood ratios can compensate. In this regime, Stockmarr’s caution applies: match evidence loses evidential weight as search populations grow. The same mathematics governs both contexts; the numerical parameters place them on opposite sides of the critical scale $n \sim \exp(\lambda D)$.

5.5 Key Takeaways

1. **Bayesian scaling mirrors frequentist scaling:** Bayesian actionability inherits the exponential factor $e^{\lambda D(c\|1)}$ but includes the additional multiplicative factor $(1 - \alpha)rs/\alpha$; see (15).
2. **Posterior collapse can precede frequentist failure:** In the sparse-target regime, posterior reliability collapses once nq approaches rs , often well before the frequentist transition at $nq \sim 1$.
3. **Exponential data growth overwhelms adaptation:** Reducing q by a factor of β requires increasing k by only $\log(1/\beta)/(pD)$, while real-world data growth is exponential: $k(t) = k_0\gamma^t$ (Section 3). Thus posterior collapse is temporally inevitable.
4. **Epistemic saturation:** As n grows, base rates $\pi = r/n$ shrink. Even rare false positives become dominated by prior odds, causing $\Pr(\text{target} \mid \text{flag})$ to decay toward zero.
5. **Resolution of the DNA debate:** Stockmarr and Balding are correct in different regimes: Balding for $nq \ll 1$ (DNA), Stockmarr for $nq \gtrsim 1$ (large-scale attribute screening).

Remark 5.4 (Connections to Classical Statistical Fallacies). This section unifies the base-rate fallacy, the prosecutor’s fallacy, false discovery rate control [Benjamini and Hochberg, 1995], and the PPV problem in medical screening [Welch and Black, 2011]. Conceptually, these phenomena are identical: all reflect Bayes’ rule under low prevalence and imperfect specificity. The widely cited argument that “most published research findings are false” [Ioannidis, 2005] is the same FDR/PPV problem in another domain.

6 Effective Dimensionality Under Correlation

Real surveillance data exhibit spatial and temporal dependencies that fundamentally alter tail probabilities. While correlation does not change the expected number of matches (by linearity of expectation, $\mathbb{E}[\sum_{i=1}^k X_i] = kp$ regardless of dependence structure), it causes *overdispersion* that inflates tail probabilities beyond the independent Poisson approximation.

6.1 Variance Inflation and Rate Function Reduction

For binary indicators X_1, \dots, X_k with $\mathbb{E}[X_i] = p$ and pairwise correlation $\text{Corr}(X_i, X_j) = \rho_{ij}$, the sum $Y = \sum_{i=1}^k X_i$ has:

$$\begin{aligned} \mathbb{E}[Y] &= kp \quad (\text{unchanged by correlation}), \\ \text{Var}(Y) &= kp(1-p) + \sum_{i \neq j} p(1-p)\rho_{ij} = kp(1-p) \left(1 + \frac{\sum_{i \neq j} \rho_{ij}}{k} \right), \end{aligned}$$

where the *design effect* $\text{DEFF} = \frac{\sum_{i \neq j} \rho_{ij}}{k}$ quantifies variance inflation; for nonnegative average correlation this satisfies $\text{DEFF} \geq 0$ [Kish, 1965].

For the Poisson approximation, independence gives $\text{Var}(Y) = \lambda = kp$. Under positive correlation, $\text{Var}(Y) > \lambda$, creating heavier tails. Positive correlation generally reduces the large-deviation rate compared to the independent case, producing heavier tails; see Dembo and Zeitouni [2010] for conditions. For intuition, one can treat the reduction in rate as shrinking the exponent by the factor k_{eff}/k .

6.2 Effective Degrees of Freedom

Rather than reducing λ itself, correlation reduces the *effective degrees of freedom* governing the concentration behavior. Standard design-effect methodology [Kish, 1965, Bretherton et al., 1999] parameterizes this through an effective sample size k_{eff} defined such that the variance of the correlated sum equals that of k_{eff} independent observations:

$$\text{Var}(Y) = k_{\text{eff}} \cdot p(1-p). \tag{17}$$

For spatial correlation with exponential decay $\rho(r) = e^{-r/\xi}$ over a monitored area A , the spatial integral of the correlation function yields:

$$k_{\text{eff}} \approx \frac{A}{2\pi\xi^2}, \tag{18}$$

where ξ is the correlation length [Bretherton et al., 1999]. Similarly, for temporal correlation with correlation time τ and unit sampling interval, the Bartlett-Wilks formula [Wilks, 2019] gives:

$$k_{\text{eff}} \approx \frac{k}{1 + 2 \sum_{h=1}^{k-1} \rho_{\text{time}}(h)(1 - h/k)}. \tag{19}$$

For exponential temporal correlation $\rho_{\text{time}}(h) = e^{-h/\tau}$ with $\tau \gg 1$:

$$k_{\text{eff}} \approx \frac{k(1 - e^{-1/\tau})}{1 + e^{-1/\tau}} \approx \frac{k}{2\tau}. \tag{20}$$

6.3 Impact on Critical Populations

We model the effect of correlation by shrinking the effective number of independent comparisons from k to k_{eff} , holding the marginal match probability p fixed. The true mean number of matches remains $\lambda = kp$, but the concentration (and hence the large-deviation exponent) behaves as if only k_{eff} coordinates contributed independently.

For thresholds $m = c\lambda$ with $c > 1$, the tail probability under correlation satisfies:

$$q_{\text{corr}} \gtrsim \exp(-k_{\text{eff}}p \cdot D(c||1)) = \exp\left(-\lambda \cdot \frac{k_{\text{eff}}}{k} \cdot D(c||1)\right). \quad (21)$$

(This expression should be interpreted as a heuristic design–effect approximation: positive dependence reduces the large–deviation rate, and replacing k by k_{eff} captures the dominant variance–inflation effect, but does not constitute a full large–deviation principle under general dependence.)

This heuristic approximation assumes that variance inflation captures the dominant effect of correlation on tail probabilities. Rigorous large-deviation analysis under general dependence is more complex [Dembo and Zeitouni, 2010], but the effective dimension approach provides useful quantitative guidance for practitioners.

This modifies the critical population scale. The exponent in the independent case $\lambda D(c||1) = kpD(c||1)$ is reduced by the factor k_{eff}/k , yielding:

$$n_{\text{crit}}^{\text{corr}} \lesssim \sqrt{\lambda} \exp\left(\frac{k_{\text{eff}}}{k} \cdot \lambda D(c||1)\right) = \sqrt{\lambda} \exp(k_{\text{eff}}p \cdot D(c||1)). \quad (22)$$

The critical population is thus *reduced* compared to the independent case, making systems fail at smaller populations when positive correlations are present. The factor k_{eff}/k represents the *information loss* due to redundancy in correlated observations.

6.4 Quantitative Examples

Example 6.1 (City-Scale Spatial Surveillance). Consider fine-grained location monitoring with $k = 10,000$ cells covering area $A = 100 \text{ km}^2$ with correlation length $\xi = 500 \text{ m}$. The effective number of independent spatial tests is:

$$k_{\text{eff}} \approx \frac{100 \times 10^6 \text{ m}^2}{2\pi(500)^2} \approx 64.$$

Despite nominally tracking 10,000 locations, correlation reduces effective information to approximately 64 independent observations.

With $p = 0.005$, the expected number of matches is $\lambda = kp = 10,000 \times 0.005 = 50$. Set the threshold at $m = 75$ matches (corresponding to $c = m/\lambda = 1.5$, validly in the upper tail regime with $c > 1$ as required by Theorem 2.4).

The rate function is:

$$D(1.5||1) = 1.5 \log(1.5) - 1.5 + 1 \approx 0.108.$$

Independent case: The exponent governing the critical population is:

$$\lambda D(c||1) = 50 \times 0.108 = 5.4,$$

giving $n_{\text{crit}} \sim \sqrt{\lambda} \exp(5.4) \approx 7.07 \times 221 \approx 1,560$.

Correlated case: By equation (22), the exponent is reduced by the factor k_{eff}/k :

$$\frac{k_{\text{eff}}}{k} \cdot \lambda D(c||1) = \frac{64}{10,000} \times 5.4 \approx 0.0345,$$

giving $n_{\text{crit}}^{\text{corr}} \sim \sqrt{\lambda} \exp(0.0345) \approx 7.07 \times 1.035 \approx 7$.

Spatial correlation reduces the critical population from approximately 1,560 to approximately 7, a reduction of over two orders of magnitude. The system can reliably monitor only a handful of individuals once spatial dependencies are properly accounted for, demonstrating how correlation-induced overdispersion dramatically accelerates false-alert saturation.

Example 6.2 (Routine Behavior Monitoring). For daily surveillance data ($\Delta t = 1$ day) over one year ($k = 365$ observations) monitoring movement patterns with correlation time $\tau = 30$ days, we obtain:

$$k_{\text{eff}} \approx \frac{k}{2\tau} = \frac{365}{60} \approx 6.$$

Observing someone’s location 365 times yields effective information equivalent to approximately 6 independent observations.

With per-observation match probability $p = 0.02$, the expected matches are $\lambda = 365 \times 0.02 = 7.3$. Set threshold $m = 12$ (giving $c = 12/7.3 \approx 1.64$). The rate function is:

$$D(1.64||1) = 1.64 \log(1.64) - 1.64 + 1 \approx 0.173.$$

Independent case: $\lambda D(c||1) = 7.3 \times 0.173 \approx 1.26$, giving $n_{\text{crit}} \sim \sqrt{\lambda} e^{1.26} \approx 2.7 \times 3.5 \approx 9.5$ (ignoring the subexponential $\sqrt{\lambda}$ factor for rough scaling gives $n_{\text{crit}} \sim e^{1.26} \approx 3.5$).

Correlated case: $(k_{\text{eff}}/k) \cdot \lambda D = (6/365) \times 1.26 \approx 0.021$, giving $n_{\text{crit}}^{\text{corr}} \sim \sqrt{\lambda} e^{0.021} \approx 2.7 \times 1.02 \approx 2.8$ (or $e^{0.021} \approx 1.02$ ignoring the prefactor).

Temporal correlation reduces the critical population from approximately 10 individuals to approximately 3, making reliable surveillance of even small groups challenging. Routine behaviors create such massive information redundancy that even year-long observation provides minimal discriminative power.

6.5 Connections to Multiple Testing

This effective dimension reduction connects surveillance analysis to multiple-testing corrections in genomics [Nyholt, 2004] and neuroimaging [Worsley et al., 1996], where similar correlation structures require Bonferroni-type corrections scaled by k_{eff} rather than the nominal number of tests k . The mathematics forces system designers to confront the limited information content of nominally “big” data: more observations do not guarantee more information when those observations are highly correlated.

Remark 6.3 (Overdispersion as System Weakness). Correlation-induced overdispersion represents a fundamental vulnerability in screening systems. Positive correlation makes extreme events (high match counts) more probable than the independent Poisson model predicts, accelerating the onset of false-alert saturation. System designers cannot escape this by collecting more data; additional correlated observations provide diminishing marginal information while accumulating the same false-positive burden. While our analysis uses effective degrees of freedom as a heuristic to quantify correlation effects, the qualitative conclusion is robust: positive correlation always weakens concentration, making false alerts more likely than independence would suggest.

7 Conclusion

We have established sharp probabilistic limits, under standard rare-event and independence (or effective-independence) assumptions, for large-scale screening systems. The critical population size beyond which false alerts become inevitable scales as

$$n_{\text{crit}} \sim \sqrt{\lambda} \exp(\lambda D(c||1)),$$

governed by large-deviation rate functions that cannot be circumvented through algorithmic refinement within these models. When data volume grows exponentially, $k(t) = k_0\gamma^t$, any screening system has a calculable operational lifetime

$$T^* \approx \frac{\log m - \log(k_0 p)}{\log \gamma},$$

typically measured in years rather than decades. Threshold adjustments provide only logarithmic protection against exponential growth, making temporal failure inevitable rather than merely possible.

The Bayesian analysis reveals an even more stringent constraint: posterior probabilities collapse when $nq \gg rs$, rendering flags epistemically meaningless well before frequentist reliability fails. This asymptotic framing clarifies the long-standing DNA database controversy: Stockmarr’s caution and Balding’s confidence apply in distinct regimes, separated by the critical scale $n \sim \exp(\lambda D)$.

Differential surveillance exposure creates exponential outcome disparities whenever common thresholds are applied across groups with heterogeneous match probabilities p_g . The mathematics guarantees disproportionate false-alert burdens through Poisson tail behavior. This is not an artifact of algorithmic bias but a structural inevitability arising from heterogeneous data collection.

These results impose non-negotiable constraints on system design. Operational surveillance systems require: (1) explicit expiration dates calculated from data growth rates; (2) demographic exposure audits measuring p_g across population groups; (3) capacity constraints limiting investible flags; and (4) recognition that system-wide reliability is dominated by the subpopulation with the highest effective match probability. The mathematics is unforgiving: more data does not guarantee better decisions, and exponential growth ensures finite operational windows.

The policy implication is direct: screening systems operating near or beyond their critical parameters will generate false alerts regardless of implementation quality. Designers must either accept these mathematical limits or fundamentally restructure surveillance architectures to avoid accumulating correlated data over time. Threshold refinement and algorithmic optimization cannot solve problems rooted in probabilistic inevitability.

Acknowledgments

We acknowledge the support of the Natural Sciences and Engineering Research Council of Canada (NSERC), [funding reference number RGPIN-2019-04085].

References

- Axelsson, S. (2000). The base-rate fallacy and the difficulty of intrusion detection. *ACM Transactions on Information and System Security*, 3(3):186–205.
- Balding, D. J. and Donnelly, P. (1995). Inference in forensic identification. *Journal of the Royal Statistical Society: Series A*, 158(1):21–38.

- Balding, D. J. (2002). The DNA database search controversy. *Biometrics*, 58(1):241–247.
- Barbour, A. D., Holst, L., and Janson, S. (1992). *Poisson Approximation*. Oxford University Press.
- Barbour, A. D. and Chen, L. H. Y. (2005). *An Introduction to Stein’s Method*. Singapore University Press.
- Barocas, S., Hardt, M., and Narayanan, A. (2019). *Fairness and Machine Learning: Limitations and Opportunities*. fairmlbook.org.
- Benjamin, R. (2019). *Race After Technology: Abolitionist Tools for the New Jim Code*. Polity Press.
- Benjamini, Y. and Hochberg, Y. (1995). Controlling the false discovery rate: A practical and powerful approach to multiple testing. *Journal of the Royal Statistical Society: Series B*, 57(1):289–300.
- Bretherton, C. S., Widmann, M., Dymnikov, V. P., Wallace, J. M., and Bladé, I. (1999). The effective number of spatial degrees of freedom of a time-varying field. *Journal of Climate*, 12(7):1990–2009.
- Chouldechova, A. (2017). Fair prediction with disparate impact: A study of bias in recidivism prediction instruments. *Big Data*, 5(2):153–163.
- Corbett-Davies, S., Pierson, E., Feller, A., Goel, S., and Huq, A. (2017). Algorithmic decision making and the cost of fairness. In *Proceedings of the 23rd ACM SIGKDD International Conference on Knowledge Discovery and Data Mining*, pages 797–806.
- Dembo, A. and Zeitouni, O. (2010). *Large Deviations Techniques and Applications*, 2nd edition. Springer.
- Dwork, C., Hardt, M., Pitassi, T., Reingold, O., and Zemel, R. (2012). Fairness through awareness. In *Proceedings of the 3rd Innovations in Theoretical Computer Science Conference*, pages 214–226.
- Eubanks, V. (2018). *Automating Inequality: How High-Tech Tools Profile, Police, and Punish the Poor*. St. Martin’s Press.
- Fawcett, T. (2006). An introduction to ROC analysis. *Pattern Recognition Letters*, 27(8):861–874.
- Feller, W. (1968). *An Introduction to Probability Theory and Its Applications*, Vol. 1, 3rd edition. Wiley.
- Hardt, M., Price, E., and Srebro, N. (2016). Equality of opportunity in supervised learning. *Advances in Neural Information Processing Systems*, 29.
- Hilbert, M. and López, P. (2011). The world’s technological capacity to store, communicate, and compute information. *Science*, 332(6025):60–65.
- Hoeffding, W. (1963). Probability inequalities for sums of bounded random variables. *Journal of the American Statistical Association*, 58(301):13–30.
- Ioannidis, J. P. A. (2005). Why most published research findings are false. *PLoS Medicine*, 2(8):e124.

- Kaye, D. H. (2013). The genealogy detectives: A constitutional analysis of familial searching. *American Criminal Law Review*, 51(1):109–163.
- Kish, L. (1965). *Survey Sampling*. Wiley.
- Lyon, D. (2003). *Surveillance as Social Sorting: Privacy, Risk, and Digital Discrimination*. Routledge.
- Mitzenmacher, M. and Upfal, E. (2005). *Probability and Computing: Randomized Algorithms and Probabilistic Analysis*. Cambridge University Press.
- Nyholt, D. R. (2004). A simple correction for multiple testing for single-nucleotide polymorphisms in linkage disequilibrium with each other. *American Journal of Human Genetics*, 74(4):765–769.
- O’Neil, C. (2016). *Weapons of Math Destruction: How Big Data Increases Inequality and Threatens Democracy*. Crown Publishers.
- Pollanen, M. (2024). A double birthday paradox in the study of coincidences. *Mathematics*, 12(24):3882.
- Robbins, H. (1955). A remark on Stirling’s formula. *The American Mathematical Monthly*, 62(1):26–29.
- Scheirer, W. J., de Rezende Rocha, A., Sapkota, A., and Boulton, T. E. (2013). Toward open set recognition. *IEEE Transactions on Pattern Analysis and Machine Intelligence*, 35(7):1757–1772.
- Schneier, B. (2015). *Data and Goliath: The Hidden Battles to Collect Your Data and Control Your World*. W. W. Norton & Company.
- Stockmarr, A. (1999). Likelihood ratios for evaluating DNA evidence when the suspect is found through a database search. *Biometrics*, 55(3):671–677.
- Storvik, G. (2006). The DNA database search controversy revisited: A hierarchical Bayesian approach. *Biometrics*, 62(3):652–661.
- Storey, J. D. (2002). A direct approach to false discovery rates. *Journal of the Royal Statistical Society: Series B*, 64(3):479–498.
- Welch, H. G. and Black, W. C. (2011). Overdiagnosis in cancer. *Journal of the National Cancer Institute*, 103(8):605–613.
- Wilks, D. S. (2019). *Statistical Methods in the Atmospheric Sciences*, 4th edition. Academic Press.
- Worsley, K. J., Marrett, S., Neelin, P., Vandal, A. C., Friston, K. J., and Evans, A. C. (1996). A unified statistical approach for determining significant signals in images of cerebral activation. *Human Brain Mapping*, 4(1):58–73.